Effects of Variable Elastic Modulus on Springback Predictions in Stamping Advanced High-Strength Steels (AHSS)

H. Kim[1)*], M. Kimchi[1)], N. Kardes[2)], T. Altan[2)]

[1)] Edison Welding Institute (EWI), Columbus / Ohio / United States; [2)] The Ohio State University, Center for Precision Forming (OSU/CPF), Columbus / Ohio / United States

* Corresponding author: E-mail address: hkim@ewi.org; Tel.: +1 614 688 5000

Abstract
In this study, the effect of variable elastic modulus on springback was investigated by using various stamping tests and finite-element method (FEM) simulation codes. The cyclic loading-unloading tensile tests were conducted to determine the variations of elastic modulus for dual-phase (DP) 600 and DP 780 sheet steels. The non-linear reduction of elastic modulus for increasing the plastic strain was formulated by using the Yoshida model that was implemented in FEM simulations for springback. To understand the effects of material properties on springback, experiments were conducted with a simple geometry such as U-shaped bending and more complex geometry such as U-flanging and S-rail stamping. The variable elastic modulus improved springback predictions in U-bending and U-flanging tests compared to FEM with the constant elastic modulus. However, in S-rail stamping tests, FEM model with the isotropic hardening model showed limitations in predicting the sidewall curl of the S-rail part after springback. To consider the kinematic hardening and Bauschinger effects that resulted from material bending-unbending in the S-rail stamping, the advanced plasticity model was attempted for FEM simulation of S-rail stamping and springback. The FEM predictions showed good improvements in correlating with experiments.

Keywords: Sheet forming, Springback, Variable elastic modulus

Introduction

Advanced high-strength steels (AHSS) has been increasingly applied for automotive structural components, allowing improvement in crashworthiness without corresponding weight increases. Forming AHSS requires much harder dies that are more expensive to rework for compensating springback. AHSS is known to have unique elastic and plastic material behaviors. This becomes more difficult for press-shop engineers and tooling designers to control or compensate for springback in their production and tooling design. Therefore, the reliable prediction and practical compensation of springback are important to allow production of the desirable stamped parts. Authors conducted the springback analyses using a simple V-die bend test and FEM in Kim et al. (2009). S-rail stamping study was conducted and the springback of S-rail parts was conducted using FEM with an isotropic hardening model and a variable elastic modulus. In this paper, particularly, a kinematic hardening model and a variable elastic modulus were used to simulate the S-rail stamping and springback to consider the Bauschinger effect and kinematic hardening of AHSS.

State of the Art

Springback behavior of sheet materials has been studied for many years. This issue became more important with the advent of AHSS. The magnitude of springback correlates with elastic modulus and the hardening behavior of sheet material. There are a number of references on modeling of springback in forming AHSS. Important references are briefly summarized here in two aspects: the effects of (i) variable elastic modulus, and (ii) non-linear hardening behavior (i.e., kinematic hardening and Bauschinger effect) on springback.

The change of elastic modulus with increasing plastic strain was investigated first by Lems (1963) and then more recently by Morestin et al. (1996) using a uni-axial tensile test during the loading process. Hildebrand et al. (2001) and Yang et al. (2004) found that the elastic modulus can be dependent on alloying elements in a microscopic view, the grain size and pile-up of dislocations near to grain boundary. Cleveland and Ghosh (2002) found that the slope of the elastic modulus variation was different during loading and unloading, and explained that the difference was due to micro-plastic strain, which did not overcome the barriers set up during forward flow nor created storage of a new dislocation network. Thibaud et al. (2004) determined the elastic modulus variation of low-alloyed transformation-induced plasticity (TRIP) steels with plastic deformation by using the vibrometric identification method which uses beam and plate vibration theories and Kwon et al. (2006) showed the variation of the elastic modulus using indentation testing. Zhu et al. (2004) found that the change in the elastic modulus decreased from 6 to 12% for mild steels and from 9 to 25% for AHSS when the strain increased from 1 to 5%.

In sheet metal forming, thorough understanding of the hardening models, which describe proper material behavior, is very important for accurate springback prediction. The mathematical theory of elastoplasticity is now well understood since several works of Hill (1950), Chaboche et al. (1990), and Khan et al. (1995). Chun et al. (2001) and Chung et al. (2005) concluded that the isotropic hardening model may not be so effective when the material undergoes non-monotonous deformations. To reproduce this Bauschinger effect, Prager (1956) and Ziegler (1959) proposed the linear kinematic hardening model, resulting in underestimating the springback because this model considers the yield surface without changing its shape and size. The cyclic hardening model of Chaboche was further improved by considering the kinematic hardening parame-

ters as functions of the effective plastic strain [Chun et al. (2002a and 2002b)] and proposing the rotational hardening model the multi-axial elastoplastic behavior [Choi et al. (2006a and 2006b)]. Yoshida et al. (2002) proposed a new material model with the consideration of the decrease in elastic modulus, transient softening, kinematic hardening, and the Bauschinger effect based on the cyclic tension-compression test at large strains for AHSS. Chen et al. (2009) conducted various case studies on lab-scale and full-scale automotive structural parts using the improved simulation technologies by considering the kinematic hardening, Bauschinger effect, smooth tool contact, and selective mass scaling. The results showed significant improvement of springback prediction compared to experiments.

From literature review, the investigation of elastic modulus variation during loading and unloading, and the development of a variable elastic modulus model that can explain this behavior adequately would improve the accuracy of springback prediction in the finite-element method (FEM). The objective of this study was to improve the prediction of springback in FE simulation of stamping AHSS parts by considering the variation of elastic modulus, kinematic hardening, and the Bauschinger effects.

Approach

In this study, springback has been evaluated by three different forming tests such as (**Fig. 1**):

- U-Bending Test (UBT) with and without stretch
- Curved-Flanging Test (CFT)
- S-Rail Stamping Test (SST)

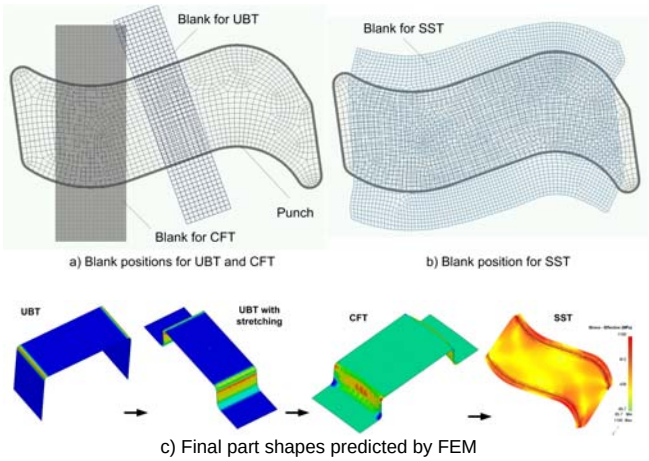

Figure 1. Schematic of various forming tests with S-shaped tooling and the final shape predicted by FEM.

Two different commercial FEM codes, LS-DYNA and DEFORM-3D, were used to analyze the experimental results and predict springback. As shown in **Fig. 1**, various stamping tests were conducted with an S-rail die at a 160-ton hydraulic press with the CNC-controlled cushion system.

Results

Characterization of material properties. The material properties of two different grades, DP 600 (0.77-mm) and DP 780 (1.0-mm) of AHSS were determined. The elastic and plastic material properties were determined by using the ASTM standard tensile test and biaxial bulge test. Three samples were tested for each condition. **Table 1** shows the material properties of DP 600 and DP 780 that were obtained from the tensile test in both rolling and transverse directions.

Table 1: Summary of ASTM tensile test results.

Sheet Material	Tensile Testing Direction	0.2% Yield (MPa)	UTS (MPa)	Total Elongation (%)
DP 600 (t_0=0.77 mm)	RD	482.4	684.5	20.1
	TD	453.8	654.5	22.8
DP 780 (t_0=1 mm)	RD	538.6	865.5	19.3
	TD	531.7	872.4	15.1

A larger range of true stress-strain data for DP 780 was obtained by conducting the viscous pressure bulge (VPB) test, because the tensile test gave a relatively small range of data. As compared in **Fig. 2**, while the tensile test reaches a maximum strain of 0.11 for DP 780, the VPB test reaches higher maximum strains, up to 0.37, which are often observed in stamping processes.

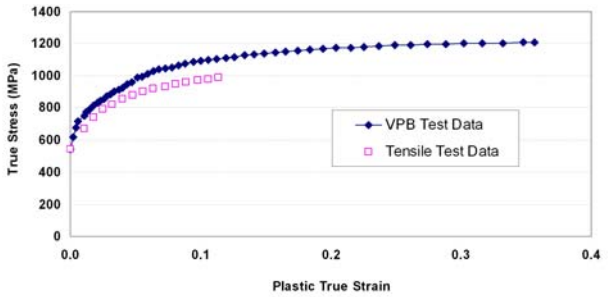

Figure 2. True stress-strain data obtained from the VPB test and tensile test for DP 780.

The cyclic loading-unloading tensile test was conducted to quantify the change of elastic modulus of DP 600 and DP 780 materials as the strain increases. The elastic modulus was obtained by calculating the slopes of loading and unloading curves, as shown in **Fig. 3**.

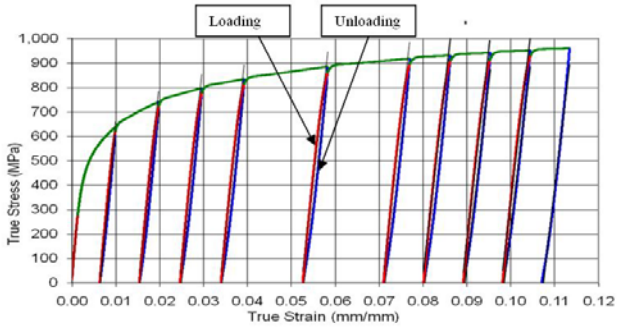

Figure 3. True stress-strain curves in the loading and unloading tensile test for DP 780 material.

The elastic modulus is more relevant to springback than the elastic loading modulus because springback takes place when the workpiece is released from the punch or die. DP 700 showed the larger reduction of elastic modulus as the true strain increased compared to DP 600. The elastic modulus of DP 780 was found to decrease about 28% from the initial elastic properties to the elastic modulus at 0.11 strain (**Fig. 4**). DP 600 showed about a 22% reduction of apparent elastic modulus from its initial value as the strain increased up to 0.14. The variation of elastic modulus during unloading was used to determine the mathematical forms of the variable elastic modulus model, the "Yoshida-Uemori model", as shown in **Fig. 4**. Three coefficients (E^0, E^A, and ζ) in the Yoshida model were determined by fitting the outputs of the model with the measured data at a 97% confidence level.

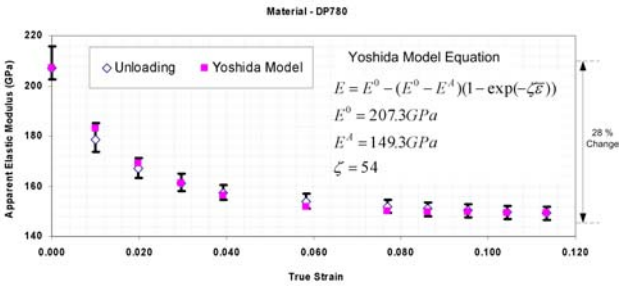

Figure 4. Yoshida model vs. experimental data for variable elastic modulus of DP 780.

Evaluation of Springback in the UBT and FEA. The UBT was conducted for DP 780 material in two different bending configurations, described as U-shaped free-bending and U-shaped stretch bending. The specimen size of 40 × 185 mm was determined by considering the straight-side edges of punch as well as the easiness to measure the bending angle of specimen side-wings.

The U-shaped free-bending test was conducted at different bending angles such as 10, 15, 25, 40, 60, and 90 degrees by controlling the die stroke. Most of the tests were conducted with no lubricant. To accurately achieve the final position of the die at different strokes, several tool-steel stoppers were placed around the stationary punch and metal shims were added on top of the stoppers to block the displacement of the die stroke mechanically.

U-shaped stretch-bending tests were conducted with the S-rail die and the blank holder. Same-sized specimens used in the U-shaped free-bending test were tested with two different blank holder forces (BHF), 2 and 8 tons. All the measurement of springback angle of tested samples was done by using an X-Y table and a high-resolution camera. Measurements were made for all the tested samples (e.g., three samples for each condition). As the BHF increased, the springback was found to decrease.

FEM analyses for the UBT were conducted by using two different commercial FEM codes, DEFORM-3D and LS-DYNA. The same input parameters of material properties, friction, and the same element size were used in both FEM codes. The coefficient of friction was defined to be 0.25, because all the experiments were conducted in a dry-friction condition (e.g., no lubricant). LS-DYNA springback simulations were run using both a variable (**Fig. 4**) and constant value (207 GPa) for the elastic modulus. The isotropic hardning model was used in simulation. The springback after U-shaped free bending was calculated by using different FEM codes. **Fig. 5** compares the FEM predictions and experiments. As the bending angle increased, the springback angle increased in the experiments. LS-DYNA with variable elastic modulus and DEFORM-3D with constant elastic modulus showed better correlations with experiments overall compared to LS-DYNA with the constant elastic modulus.

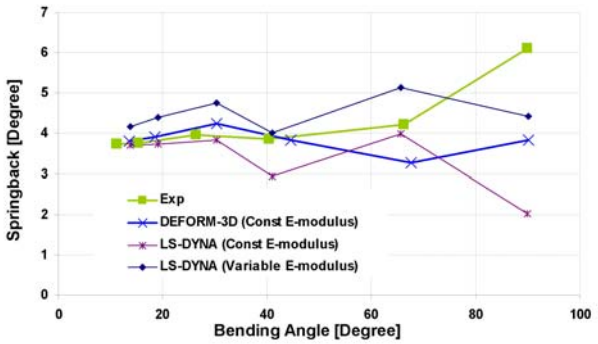

Figure 5. Comparison of springback between FEM predictions and experiments of DP 780 in U-shaped free bending.

U-shaped stretch bending was also simulated. Two LS-DYNA simulations considered both the variable elastic modulus and the constant elastic modulus. Two different springback angles in the channel opening angle (Springback 1) and the flange angle (Springback 2) were compared between FEM predictions and experiments. The comparison of springback in U-shaped stretch bending at a BHF of 2-tons is given in **Fig. 6**. In the BHF 2-ton, LS-DYNA with variable elastic modulus showed the best correlations with experiments, while DEFORM-3D and LS-DYNA with the constant elastic modulus showed similar predictions and both results gave about 4 to 5 degrees error with respect to experiments.

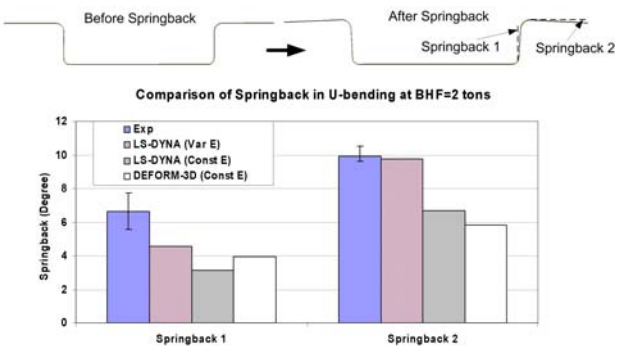

Figure 6. Comparison of springback in U-shaped stretch bending of DP 780 at a BHF of 2 tons.

Evaluation of Springback in the CFT and FEA. The springback was investigated with the CFT. In the CFT,

non-uniform stress and strain conditions cause 3-D geometric changes such as variations of channel opening and side-wall curls, as well as twisting of the drawn channel. The effects of CFT were investigated with tests conducted at two different BHF levels.

The CFTs were conducted for DP 780 with an S-rail die by placing the rectangular sample (60 × 185 mm) with respect to the S-rail punch. Most of the experiments were conducted without lubricant. The six different angles on the tested specimens which were measured are shown in **Fig. 7**.

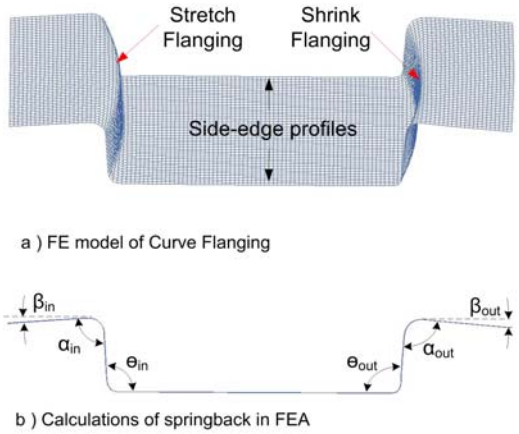

Figure 7. Locations of the measurements for various angles after springback.

The mid-section profile was difficult to accurately measure using the camera system or the manual-type protractor. Therefore, the side-edge profiles of tested samples were measured and the average value of measured angles was used to quantify springback.

Final bending angles of FEM predictions and experiments at 8-ton BHF are compared in both **Fig. 8** and **Fig. 9**. The variable elastic modulus gave better predictions of the flange angles, β_{in} and β_{out}. However, for the channel angles (θ_{in} and θ_{out}) and the shoulder angles (α_{in} and α_{out}), it is not clear which elastic modulus model gave better predictions compared to experiments. This may be caused by possible measurement errors for these angles. It was more difficult to accurately measure the channel angles and the shoulder angles compared to the flange angles, because of the sidewall curl and twisting.

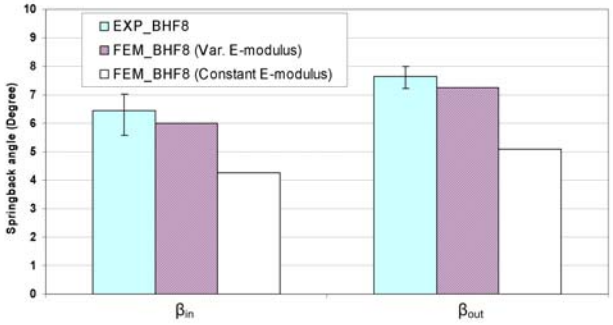

Figure 8. Comparison of springback angle in the flange areas between FEM predictions and experiments.

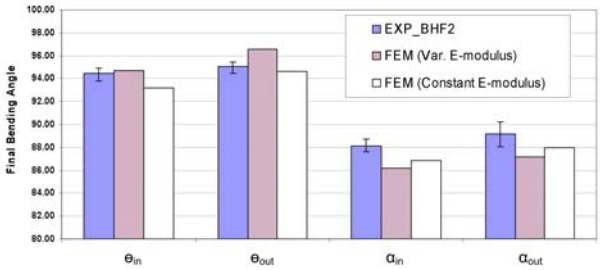

Figure 9. Comparison of the final bending angles of curved flanging between FEM predictions and experiments at a BHF of 8 tons.

Evaluation of Springback in the SST and FEA.. In the SST, the distributions of stress and strain on the part are more complicated than for UBT and CFT. Because of complex geometry and stress conditions, three different types of springback, defined twisting of the channel, channel opening, and sidewall curl, occur in S-rail stamping. Experiments were conducted with DP 600 (t_0=0.77 mm) and DP 780 (t_0=1.0 mm) materials. The blank size and shape were determined based on preliminary FEM simulations. **Fig. 10** shows the stamping test setup and the CAD models of the initial blank geometry and the designed stamping geometry.

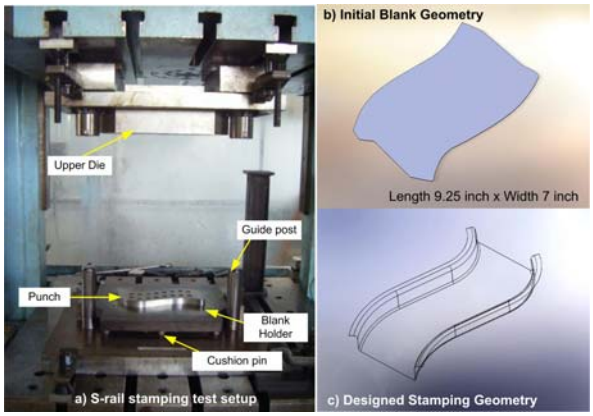

Figure 10. S-Rail tooling and the geometries of the initial blank and final stamping.

In the test, the maximum depth of stamping was determined to be 20 mm to avoid any cracking. The BHF was limited to 2 tons for both DP 600 and DP 780. A pressure pad force on the top of the hat surface was measured to be increased from 10 to 44 kN as the stroke increase up to 20 mm during stamping. The initial blanks were lubricated with a stamping lubricant before the test.

The stamped part was scanned by the 3-D white light scanning method to obtain a 3-D CAD model from the actual stamped part. **Fig. 11** shows the colored error contours (i.e., the normal-direction deviations of stamping part from the designed part geometry). DP 600 showed larger errors compared with the desirable part geometry than DP 780 based on greater errors in the channel opening and twisting. The thinner sheet material usually experiences more springback. DP 600 is 23% thinner than DP 780.

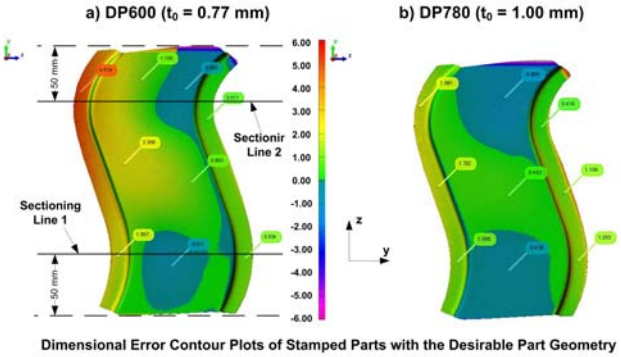

Figure 11. Springback measurements for DP 600 and DP 780 stampings with the designed part geometry (all dimensions shown are in millimeters).

FEM simulations for S-rail stamping were conducted by using a commercial FEM code, LS-DYNA. Two different elastic modulus models; a constant (207 GPa) and the variable (as given in **Fig. 4**); two different hardening models; the isotropic hardening and kinematic hardening models; were used for DP 780 in the FEM simulations. Shell elements with a 2-mm element size were used for the sheet blank model. The coefficient of friction was input as 0.125 between the workpiece and the punch or die. As shown in **Fig. 12**, the FEM model was carefully set up by considering the relative positions of the initial sheet blank to other punches and dies, which were measured in the experiments.

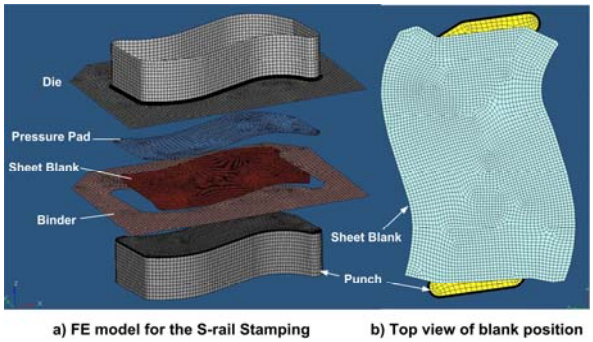

Figure 12: S-Rail stamping simulation model and the configuration of the initial position of blank.

The isotropic hardening model did not provide accurate results of springback regardless of elastic modulus models; a constant or variable. The detailed results have been published in Kim et al. (2009). Therefore, in this study, the Yoshida-Uemori model [Yoshida and Uemori, 2002] was used to consider the effects of the kinematic hardening and the Bauschinger effect on springback. This model was implemented by using an advanced material model (*MAT_125) that is available in LS-DYNA [LSTC 2010]. The detailed parameters for DP 780 were provided by a steel supplier [Chen et al. 2009], as shown in **Table 2**.

Two different sections on the stamping were compared for springback between the actual and FEM predicted final part geometry as shown in **Fig. 13**. Two reference points at the top flat sectional profile were fixed to compare the multiple profiles together.

Table 2: Parameters for the Yoshida-Uemori model for DP 780

Variable	CB	Y	SC	K	RSAT	SB	H
Value	453 MPa	291 MPa	513 MPa	62	700 MPa	449 MPa	0.95
Variable	EA	COE	IOP	C1	C2		
Value	149 GPa	54	0.0	0.052	0.955		

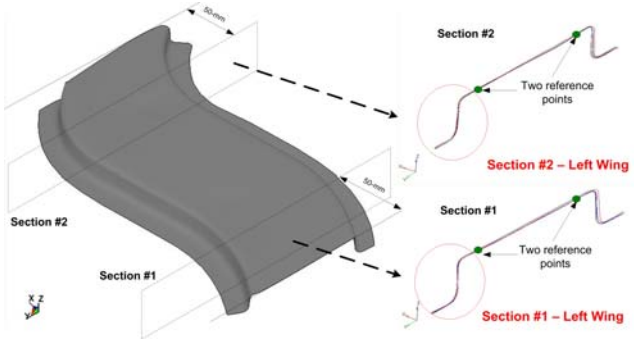

Figure 13: Two selected sections for springback comparison.

Fig. 14 compares springback results for two different sections. New simulation results (A and B); using the Yoshida-Uemori model showed better correlations with experiments (Exp) compared to the isotropic hardening model results (C and D). The variable elastic modulus (A) gave better predictions of the channel opening (θ) and the flange angle (β), while the constant elastic modulus showed slightly better correlation with experiment for the die-shoulder angle (α).

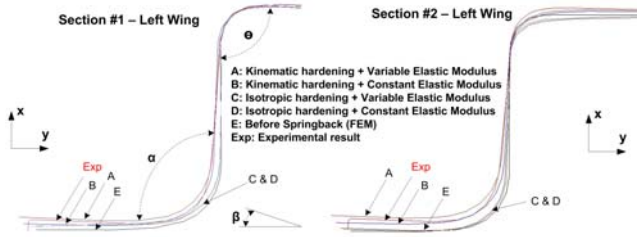

Figure 14: Comparison of FEM predictions and experiment.

Discussion

The scientific contribution of this study is to predict springback in a S-rail stamping by considering the unique material behaviors such as the variation of elastic modulus, and the kinematic hardening and Bauschinger effect observed in AHSS using a commercial FEM code. To verify the effectiveness of Yoshida model in predicting springback for other AHSS, additional study with TRIP and TWIP steels is required for future work.

Conclusion

The following conclusions can be drawn from this project:

- As the plastic strain increases, the elastic modulus significantly decreased up to 22% for DP 600 and 28% for DP 780 from the initial values.

- FEM with the variable elastic modulus showed better agreements with measured springback at different bend angles in the U-shaped bending test Compared to FEM with a constant elastic modulus.
- The springback decreased with increasing BHF from 2 to 8-tons, as confirmed in the CFT and the U-shaped stretch bending results. However, the sidewall curl was increased for increasing the BHF.
- The isotropic hardening models with constant and variable elastic modulus showed some limitations in SST to predict the channel opening and the sidewall curl compared with experiments.
- The Yoshida-Uemori model with the consideration of kinematic hardening and the Bauschinger effects showed better correlations with springback measurements compared to the isotropic hardening models regardless of the elastic modulus models.
- To predict the springback of the relative simple part geometry; V-die or U-die bending; the constant elastic modulus and the isotropic hardening model can be reasonable input data of FEM.
- However, to predict the spingback of the complicate part geometry, it is recommended to define the nonlinear hardening behaviors and elastic modulus change in the material input data for reliable FEM simulations.

Acknowledgements

This project was conducted with support from the State of Ohio, Department of Development, and Thomas Edison Program. The author would like to thank Dr. Boel Wadman, Project Manager of Swerea-IVF, for her support and advice on this research program.

References

Chaboche, J. L. and Lemaitre, J. 1990. Mechanics of solid materials, Cambridge University Press.

Chen, X., Shi, M., Zhu, X., Du, C., Xia, Z.C., Xu, S., Wang, C.T., 2009. Springback prediction improvement using new simulation technologies, SAE Paper 2009-01-0981.

Choi, Y., Han, C. S., Lee, J. K., and Wagoner, R. H. 2006a. Modeling multi-axial deformation of planar anisotropic elasto-plastic materials, part I: theory, Int. J. Plasticity 22, p. 1745-1764.

Choi, Y., Han, C. S., Lee, J. K., and Wagoner, R. H. 2006b. Modeling multi-axial deformation of planar anisotropic elasto-plastic materials, part II: application, Int. J. Plasticity 22, p. 1765–1783.

Chun, B. K. 2001. Study on hardening models and numerical implementation for spring-back prediction, Ph.D. Dissertation, The Ohio State University.

Chun, B. K., Jinn, J. T., and Lee, J. K. 2002a. Modeling the Bauschinger effect for sheet metals, part I: theory, Int. J. Plasticity 18, p. 571-595.

Chun, B. K., Jinn, J. T., and Lee, J. K. 2002b. Modeling the Bauschinger effect for sheet setals, part II: applications, Int. J. Plasticity 18, p. 597-616.

Chung, K., Lee, M. G., and Kim, D. 2005. Spring-back evaluation of automotive sheets based on isotropic-kinematic hardening laws and non-quadratic anisotropic yield functions part I: theory and formulation, International Journal of Plasticity 21, p. 861-882.

Cleveland, R. and Ghosh, A. 2002. Inelastic effects on springback in metals, Int J. of Plasticity. 18, p.769-785.

Hildebrand, H. and Hildebrand, M. 2001. Microstructural influences on Young's modulus for Fe-V-C and Fe-Mo-C alloys, Mat. –wiss. u. Werkstofftech 32, p. 701-711.

Hill, R. 1950. The mathematical theory of plasticity, Oxford University Press, Oxford.

Khan, A. and Huang, S. H. 1995. Continuum theory of plasticity, John Wiley & Sons, New York.

Kim, H., Kimchi, M., and Altan, T. 2009. Control of springback in bending and flanging advanced high-strength steels (AHSS), International Automotive Body Congress (IABC), 4-5 November, Troy, MI.

Kim, H., Kimchi, M., Kardes, N., Demiralp, Y., Mete, O., Altan, T. 2010. Predictions of springback in the S-rail stamping of AHSS using FEM with the variable elastic modulus, IABC, 3-4 November, Troy, Michigan, USA.

Kwon, D. I., Lee, K. W., Kim, J. Y., and Kim, K. H. 2006. IIT-new non destructive on-site technique for estimating tensile properties, residual stresses, and fracture toughness, Proceedings of US-Korea Conferece on Science, Technology, and Entrepreneurship(UKC), Teaneck, NJ.

Lems. W. 1963. The change of Young's modulus after deformational low temperature and its recovery, Ph.D. Dissertation, Delft.

LSTC, 2010. LS-DYNA Keywords User's Manual, Vol. 2, Material Models, Version 971,Rev 5.0, p. 479-482.

Morestin, F. and Boivin, M. 1996. On the necessity of taking into account the variation in the Young's modulus with plastic strain in elastic-plastic software, Nuclear Engineering and Design 162, p. 107-116.

Prager, W. 1956. A new method of analyzing stresses and strains in work-hardening solids, ASME Journal of Applied Mechanics 23, p. 493-496.

Thibaud, S., Boudeau, N., and Gelin, J.C. 2004. Coupling effects of hardening and damage on necking and bursting conditions in sheet metal forming, Int. J. of Damage Mechanics 13, p. 107-122.

Yang, M., Akiyama, Y., and Sasaki, T. 2004. Evaluation of change in material properties due to plastic deformation, J. of Materials Processing Technology 151, p. 232-236.

Yoshida, F., Uemori, T., 2002. A model of large-strain cyclic plasticity describing the Bauschinger effect and workhardening stagnation, International Journal of Plasticity 18, p. 661-686.

Zhu, H., Huang, L., and Wong, C. 2004. Unloading modulus on springback in steels, Society of Automotive Engineering, Society of Automotive Engineering (SAE).

Ziegler, H. 1959. A modification of Prager's hardening rule, Quarterly of Applied Mathematics 17, p. 55-65.